ISSN 1330-3651 (Print), ISSN 1848-6339 (Online)
https://doi.org/10.17559/TV-20221010215018
Orginal scientific paper

Analysis of Transitional Occurrences of Low Voltage Welding Transformer

Ivan PETROVIĆ*, Marinko STOJKOV, Damir ŠLJIVAC, Mijat SAMARDŽIĆ

Abstract: The purpose of this paper is to demonstrate and analyse transition events that occur when the loaded transformer is turned on and off within the welding device. The purpose of the welder is to provide a high quality and stable voltage during the ignition of the arc, and often during the ignition of the arc the transformer comes from its no-load state to the work-load state, depending on the diameter of the electrode that the arc melts. The welding currents of the MIG/MAG (Metal Inert/Active Gas) process are not less than 100 A, about 350 A, at a voltage of the arc of 35 V (DC). In this paper, the MATLAB/PSB programme package is used to analyse the no-load inrush currents and the loaded inrush currents of welding transformers. Current and voltage waveforms were recorded on the primary side of the transformer, as well as the harmonic content of the transformer primary currents, with indicator calculation of the current waveform distortion - THDi.

Keywords: inrush currents; MATLAB; Numerical simulation; THDi; welding device transformer

1 INTRODUCTION (Introductory remarks)

At the end of 1950s and during the 1960s there was a sudden development of semiconducting components (thyristors and bipolar transistors). Semiconducting energetic electronic converters also occurred, be it directly or indirectly because of the transformers. Due to its continuous nature, they represent nonlinear network consumers and generate the occurrence of distortion to wave current form and voltage [1].

Using mathematical analysis, it is shown that distortion to waveforms, i.e., Fourier series that these distorted forms can represent a set of sinusoidal functions off different frequencies. These frequencies are an integer product of basic frequency and frequency of the analysed signal and are called higher harmonics [2]. This paper emphasises the occurrences of higher harmonic components in the electromagnetic network due to nonlinear customers are energetic converters (rectifier, inverters, …). Installed in electric installations, rectifiers are main sources of higher harmonics. Due to a high presence of nonlinear converters in the network, analysis of electrical energy quality and its constitutive part - analysis of higher harmonics affords more and more importance for economic reasons.

Distributors of electrical energy are faced with two diametrically contrary demands. On one side, electronic equipment requires a high-quality sinusoidal voltage shape, while on the other side that same equipment inserts harmonic components into the network, i.e., non-sinusoidal current which in that way diminishes electric energy quality. the role of current source regarding electric-arc welding is to adjust the network voltage to the level which enables safe establishment of the electric arc where the possibility of changing arc features is important [2].

Welding device consist of a three -phase or a monophasic transformer with rectifier diodes, regulation circuit (regulators for conditioning appropriate work parameters) and a silencer in the DC circuit.

Three-phase transformer is symmetrically stressed in all three phases of the electric network. It is usually turned on unmanaged and followed by great asymmetries of magnetic flows in the iron core. As a consequence, there are great distortions to waveform of magnetising currents. These great inrush currents effect on the power network as well as higher harmonics [3, 4].

1.1 Occurrence of Inrush Currents

Magnetic flaw in the transformer core is proportional to the power voltage integer, which means that it lags it by 90°. If the transformers is fitter in the moment when the voltage passes zero, the maximal magnetic flow is twice as big as the denominator and the leftover magnetic flow is also added to that. Amplitude of the flow possesses a DC component the duration of which depends on work and inductive circuit resistance [7].

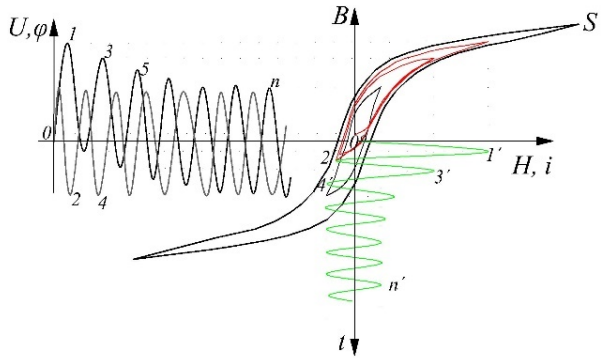

Figure 1 Depiction of dependence of electric and magnetic values in a nonlinear magnetic circuit and a principal depiction of the formation of inner magnetisation pathway [4]

Fig. 1 depicts the dependence of electrical and magnetic values in a nonlinear magnetic circuit and a principal depiction of magnetisation pathway. Maximal flow is marked with point 1. As the derivation of the magnetic flow changes at the point, that point belongs to the peak of appropriate magnetisation pathway and the appropriate magnetisation pathway, and the appropriate current of magnetisation is marked with 1'. As consequence of extreme saturation the ratio of inrush current and rated current of magnetisation is several times greater than the ratio of impact flaw at the switching and rated current of magnetisation is several times greater than the ratio of impact flow at the switching and rated magnetic flaw. If the leftover magnetism is B_0 the magnetism pathway starts from point 0 with belonging coordinates $H = 0$, $B = B_0$. If

the increment of magnetic induction is positive the magnetism pathway is formed via approaching the upward branch of the full saturation hysteresis loop. The example of the described algorithm is reached in point 2 when the increment sign of magnetic induction is changed once more, as well as the direction of magnetisation pathway [5].

While implementing an unloaded three-phase transformer into the network, the idling current i_0 occurs and it consists of t_s working component i_{0r} and significantly greater barren component i_μ [9].

In its settled state the idling current amounts to several percentages of the transformer rated current, while during implementation to the establishment of a new settled system, the component of magnetisation current can grow to values much greater than the rated current [10].

Inrush current is magnetisation current which occurs while incorporating an unloaded transformer into the electrical network [11]. The current amplitude can be multiple times greater than the rated current amplitude, and its duration is characterised with time τ_{50} which is necessary for the current to fall to half of its value. Fig. 2 showcases characteristic appearance of inrush current of incorporating an unloaded transformer.

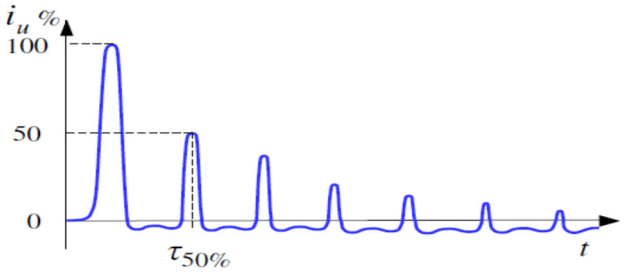

Figure 2 Characteristic appearance of the inrush current [14]

Inrush current occurs due to nonlinearity of the magnetisation curve of the iron core, in accordance with the Faraday law while the remanent magnetism can increase in further period [18]. If the transformer is incorporated when the voltage is maximal, i.e., when the stationary magnetic flow is equal to zero the inrush current is equal to the stationary idling current. Input sinusoidal voltage also conditions the sinusoidal change to the magnetic flow.

The greatest inrush current amplitude occurs when transformer is switched on in time moment when voltage is equal to zero. In that case, at the same time the remanent magnetic flow Φ_R has opposite sign in comparison to the relative value of induces magnetic flow. Due to the core saturation and great rated magnetic induction, the greatest value of the magnetism current will occur in that case [12].

1.2 Mathematical Model of Incorporating a Three-Phase Transformer

Mathematical model of three-phase transformer is the most frequently used type of transformer, a three-pillar model with primary coils connected into a star [5, 6]. Secondary part of the coil is connected to the rectifier part which is unloaded in the case of idling which the most unfavourable case forms the standpoint of surge inrush currents.

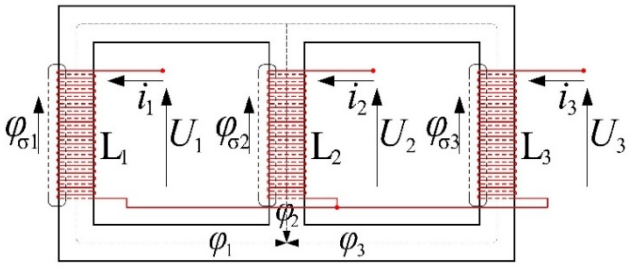

Figure 3 Simplified schematic of the idling three-phase transformer

Circuit equations for the mentioned transformer are:

$$u_1 = Ri_1 + N\frac{\varphi_1 + \varphi_{\sigma 1}}{\mathrm{d}t} = Ri_1 + N\frac{\mathrm{d}\varphi_1}{\mathrm{d}t} + L_\sigma \frac{\mathrm{d}i_1}{\mathrm{d}t} \tag{1}$$

$$u_2 = Ri_2 + N\frac{\varphi_2 + \varphi_{\sigma 2}}{\mathrm{d}t} = Ri_2 + N\frac{\mathrm{d}\varphi_2}{\mathrm{d}t} + L_\sigma \frac{\mathrm{d}i_2}{\mathrm{d}t} \tag{2}$$

$$u_3 = Ri_3 + N\frac{\varphi_3 + \varphi_{\sigma 3}}{\mathrm{d}t} = Ri_3 + N\frac{\mathrm{d}\varphi_3}{\mathrm{d}t} + L_\sigma \frac{\mathrm{d}i_3}{\mathrm{d}t} \tag{3}$$

where the following represents: N - number of the twists in the primary coil; R - working resistance of the primary coil; L_σ - leakage inductance of the primary coil.

Vectors u, i and φ represent voltage, current and magnetic flow. Each magnetic pillar is corespondendent to one flow φ_1, φ_2, φ_3.

For coil industances, refer to the following expressions:

$$L_1 = L_{\sigma 1} + L_{\varphi 1} \tag{4}$$

$$L_2 = L_{\sigma 2} + L_{\varphi 2} \tag{5}$$

$$L_3 = L_{\sigma 3} + L_{\varphi 3} \tag{6}$$

where $L_{\sigma 1}$, $L_{\sigma 2}$, $L_{\sigma 3}$ represent the leakage inductances of coils 1, 2 and 3, and $L_{\varphi 1}$, $L_{\varphi 2}$, $L_{\varphi 3}$ represent the main coil inductance.

Voltage equations in the matrix form which describe the model of the three-phase transformer used in the simulation model for analysing the inrush current:

$$[u] = [R]\cdot[i] + [L]\cdot\frac{\mathrm{d}}{\mathrm{d}t}[i] \tag{7}$$

If the matrix Eq. (7) is expanded according to its components of voltage, resistance, current and inductansce, what follows is an equation which represents the model of the three-phase transformer:

$$\begin{bmatrix} u_{11} \\ u_{12} \\ u_{13} \\ u_{21} \\ u_{22} \\ u_{23} \end{bmatrix} = \begin{bmatrix} R_{11} & 0 & 0 & 0 & 0 & 0 \\ 0 & R_{12} & 0 & 0 & 0 & 0 \\ 0 & 0 & R_{13} & 0 & 0 & 0 \\ 0 & 0 & 0 & R_{21} & 0 & 0 \\ 0 & 0 & 0 & 0 & R_{22} & 0 \\ 0 & 0 & 0 & 0 & 0 & R_{23} \end{bmatrix} \cdot \begin{bmatrix} i_{11} \\ i_{12} \\ i_{13} \\ i_{21} \\ i_{22} \\ i_{31} \end{bmatrix} + \begin{bmatrix} L_{11} & L_{12} & L_{13} & L_{14} & L_{15} & L_{16} \\ L_{21} & L_{22} & L_{23} & L_{24} & L_{25} & L_{26} \\ L_{31} & L_{32} & L_{33} & L_{34} & L_{35} & L_{36} \\ L_{41} & L_{42} & L_{43} & L_{44} & L_{45} & L_{46} \\ L_{51} & L_{52} & L_{53} & L_{54} & L_{55} & L_{56} \\ L_{61} & L_{62} & L_{63} & L_{64} & L_{65} & L_{66} \end{bmatrix} \cdot \frac{\mathrm{d}}{\mathrm{d}t} \begin{bmatrix} i_{11} \\ i_{12} \\ i_{13} \\ i_{21} \\ i_{22} \\ i_{23} \end{bmatrix} \tag{8}$$

where R_{11}, R_{12} and R_{13} represent the resistances of primary, and R_{21}, R_{22}, R_{23} the resistances of secondary coils, L_{11} to L_{66} represent the inductances of each particular coil, and L_{ij} represent the inductances between coils.

1.3 Analytical Calculation of Inrush Current

The first analytical calculation for determining maximal inrush current is given by Specht [11] and is calculated as follows (9):

$$i = -\frac{\sqrt{2}\cdot U\cdot X}{Z^2}\cdot \left[\frac{R}{X}\cdot\sin(\omega t)-\cos(\omega t)+\mathrm{e}^{-\frac{R}{X}(\omega t+\theta)}\left(\frac{R}{X}\cdot\sin\theta+\cos\theta\right)\right] \quad (9)$$

where the following represents: U - power voltage of transformer, primary side, V; X - inductive transformer resistance, Ω; R - Ohm resistance of transformer threads, Ω; Z - transformer impedance, Ω.

Angle θ is described with the following Eq. (10):

$$\theta = \cos^{-1}\left(\frac{B_s - B_r - B_m}{B_m}\right) \quad (10)$$

where the following represents: B_s - total magnetic induction of the saturated core T; B_m - peak induction value in the scroll connected to the voltage E.

Holcomb gives a simplified version of the Specht Eq. (9) for calculating the inrush current and it follows (11):

$$i = \frac{\sqrt{2}E}{\sqrt{R^2+\omega^2L^2}}\left[\sin(\omega t-\psi)-\mathrm{e}^{-\frac{R}{L\left(\frac{\theta_{sn}}{\omega}\right)}}\cdot\sin(\theta_{sn}-\psi)\right] \quad (11)$$

where the following represents: Ψ - phase angle between voltage and current determined by the equation, and it derives from the Eq. (12):

$$\psi = \tan^{-1}\left(\frac{L}{R}\right) \quad (12)$$

1.4 Specificities of Inrush Current and Its Effect on the Network and Device Where it Occurs

Problems caused by inrush currents can cause failures or errors in activity of the fuse, protective relays, or other parts of protections in the energetic system. Impact currents of the switching can also cause mechanical failures. Maximal value of inrush current can be greater in its value than the rated transformer current, and it is possible for inrush current of the switching to amount even to 90% short circuit current [11].

Value of inrush current depends on the moment of engaging and remanent magnetism in the core. During the first engaging (without remanence), the current is the lowest in the phase where the voltage is maximal, and it is the greatest in the phase where voltage is zero at the moment of engaging.

In the worst case and with the addition due the remanent magnetism, the inrush current can reach up to 40 times greater than the rated current. If the transformer is often used, rated current can cause isolation breach because accidental incorporation can happen in the moment when inrush current has the greatest value which corresponds to the moment of engaging when the phase voltage is equal to zero [13].

If transformer is often included in the circuit, isolation breach can occur due to the inrush current [14, 15].

2 CONSEQUENCE OF HIGHER HARMONICS IN THE NETWORK

All components of the energy system, as well as consumers which are incorporated to the electro-energetic system imply sinusoidal shapes of voltage and current, so every occurrence of higher harmonics has negative effects [16, 25]. Negative effects that occur because of higher harmonics:

1. Occurrence of resonance in the network,
2. Effect on condensation batteries,
3. Effect on protection elements,
4. Effect on accuracy of standard measuring instruments,
5. Additional losses in electrical machines,
6. Effect on telecommunication signals.

2.1 Occurrence of Resonance in the Network

The presence of capacitance in the network can cause the occurrence of local resonance [16]. That causes the occurrence of overly great currents and in increase in voltage. Such a state leads to failures, most often on the condensers themselves, as well as on other parts of the system. There is a serial and parallel resonance.

Serial resonance occurs when a condenser battery is parallelly connected to the consumer. It has small impedance and great voltage.

Parallel resonance occurs in more cases, and most often if the condenser is on the same busbar as the harmonic source. In that case great value of impedance and great value of voltage occur [16].

2.2 Effect on Condensation Batteries

Condensers, which make up the condenser batteries for remedying the strength factor or are within the filter system or occur in some other circuit, are in danger from the occurrence of overvoltage or great current values. The presence of harmonics within the voltage causes additional losses:

$$P_g = \sum_{n=1}^{\infty} c\tan(\delta)\cdot\omega_n\cdot U_n^2 \quad (13)$$

where the following represents: C - condenser capacitance.

$$\tan\delta = R\cdot\omega\cdot C \quad (14)$$

$$\omega_n = 2\cdot\pi\cdot n\cdot f \quad (15)$$

U_n - efective value of the *n-s* voltage harmonic.

Serial and parallel resonance between the condenser and the rest of the network causes overvoltage and high current values which increases losses, as well as overheating of the condenser which leads to shortened lifespan or dielectric breach. Therefore, condensers are made in accordance with different standards which define different levels of current strain [16].

2.3 Effect on Protective Elements

The presence of harmonics in the network is a frequent cause of errors for managing signals which manage the protective elements or are used for remote control and managing.

Negative effects manifest in improper function of the receiver, as well as possible failures on the equipment [16].

2.4 Additional Losses in Electrical Machines

Regarding transformers, the presence of voltage harmonics increases the hysteresis and loses due to eddy currents, as well as isolation strain. The flow of current harmonics increases copper losses, i.e., Joule losses. Especially pronounced are losses in triangle coils, due to harmonic circulation, currents that are multiples of 3 so that needs to be anticipated while planning (especially if a rectifier transformer is in question). Effect of higher harmonics is expressed using a Field factor which is used to increase (multiply) the expression for active loss strength. For higher *h* harmonics, expression for active loss strength becomes [16]:

$$P_{\mathrm{dod}(h)} = k_{\mathrm{F}(h)} \cdot R_{\mathrm{dc}} \cdot i_{(h)}^2, k_{\mathrm{F}(h)} \geq 1 \tag{16}$$

where the following represents: $k_{\mathrm{F}(h)}$ - Field factor; R_{dc} - Ohm resistance of the DC current; $i_{(h)}$ current value of the *h* harmonic.

In electrical rotational machines, there are two effects: increased losses and parasitic moments. Losses due to the presence of higher harmonics occur both in rotary and stationary circuit, as well as in ferromagnetic. In rotary and stationary conductors, losses can be greater due to resistance, eddy currents and the skin effect. In ferromagnetic, they contribute to increased loss of iron [16].

3 METHODS FOR REDUCING OR ELIMINATING HIGHER HARMONIC

Higher harmonics are always present within the network in a greater or smaller percentage. However, at a particular moment they can become a problem. That happened if the source of the harmonics if large, if the pathway of harmonics current is overly long, i.e., if reactance of the circle is large or if system response is such that it leads to harmonics strengthening (resonance). To lessen or eliminate the harmonic problem, there are several fundamental methods [17]:

1. Lowering the intensity of harmonic currents,
2. Filter implementation,
3. Change of the system resonant frequency.

3.1 Lowering the Intensity of Harmonics Currents

Methods of lowering the intensity of harmonic currents imply changing the working principle of plants that generate harmonics. It is change in network topology which is hard to perform in practise as it can affect the entire manufacturing process. Solution to the problem can be implemented during the designing process.

The second way of lowering harmonic current intensity is transformer coil triangle junction which leads to further blocking of all harmonics that are multiples of 3.

Imputing the 30-degree phase shift, connecting transformer minor into a star and triangle, one obtains the effect of a 12-pulse rectifier, i.e., 5^{th} and 7^{th} harmonic are eliminated [17].

3.2 Change of the System Resonant Frequency

This method is most frequently used when there are condensation batteries for reactive energy compensation are present within the system or the consumer. Their resonant frequency is often close to the frequency of typical harmonics, so there are unsolicited negative effects. The problem is often solved by changing the size of the condenser, adding serial impedance, moving the condenser to the other coil or by complete removal of the condenser from the network [16].

3.3 Filter Implementation

The goal of filter implementation is to ensure lower impedance to prevent higher harmonics to spread throughout the network.

That is the reason filters are most frequently implemented parallelly to the consumer and have a condenser with an additional stifler. Resonant filter frequency is always calculated to be slightly below the dominant harmonic frequency [17].

There are passive and active filters. Passive filters are mostly implemented parallelly to the harmonics source. Disadvantage of this type of filters is their own capacity and inductivity which can lessen resonant frequency, as well as worsening resonance prerequisites. The effect of dielectrics aging is also pronounced as its consequence is lowered condenser capacity, i.e., an increase in resonant frequency [18].

3.3.1 Dimensioning of Passive Filters

Parameters of a passive filter should be adjusted in a way that the filter represents a small impedance for a particular harmonic component and that while doing so, there is optimal compensation of reactive power.

For determining *RLC* parameters of the resonant filter with one resonant frequency, first it is necessary to determine a dominant higher harmonic which needs to be stifled. For the filter to represent smaller impedance at the frequency at which the harmonic needs to be stifled, choice of the parameters needs to ensure that resonant frequency of *RLC* filter branch be equal to frequency of the harmonics which need to be stifled [19]:

$$\omega_r = \frac{1}{\sqrt{L \cdot C}} = \omega_h \tag{17}$$

where h represents rank of the harmonic that needs to be stifled, and L and C are parameter of the *RLC* branch.

The second equation necessary for determining *RLC* filter elements with one resonant frequency refers to the factor of filter quality (in this case stiflers used in the filter). Quality factor Q_z is:

$$Q_z = \frac{\omega_r \cdot L}{R} \tag{18}$$

For resonant filters, the rotation of values for the quality factor $30 < Q_z < 60$, and in calculations it is recommended to adopt the value of $Q_z = 50$.

Third equation that is necessary for determining the *RLC* filter element is reached from the prerequisite that using the filter enables for compensation of reactive power. For deriving this prerequisite, it is necessary to determine the susceptance of resonant filter at the basic frequency ω_1. Admission of resonant filter at the basic frequency ω_1 is:

$$Y_i(\omega_1) = \frac{1}{R + j\omega_1 \cdot L + \frac{1}{j\omega_1 \cdot C_1}} \tag{19}$$

Susceptance of the resonant filter at the basic circular frequency ω_1 is:

$$B_f = Im\left\{Y_f(\omega_1)\right\} = \frac{\omega_1 \cdot C\left(1 - \omega_1^2 \cdot L \cdot C\right)}{(\omega_1 \cdot R \cdot C)^2 + (1 - \omega_1^2 \cdot L \cdot C)^2} \tag{20}$$

Using Eqs. (18) and (19), it follows:

$$B_f = \frac{\omega_1 \cdot C\left(1 - \frac{\omega_1^2}{\omega_r^2}\right)}{\left(\frac{1}{Q_z} \cdot \frac{\omega_1^2}{\omega_r^2}\right)^2 + \left(1 - \frac{\omega_1^2}{\omega_r^2}\right)} \tag{21}$$

Prerequisite of using the filter to achieve reactive power compensation implies that at the basic frequency, susceptance of the *RLC* filter branch is equal to susceptance of the condenser with optimal capacitance C_{opt} for reactive power compensation which would be used instead of the filter:

$$B_f(\omega_1) = \omega_1 \cdot C_{\text{opt}} \tag{22}$$

Based on the previous equation, the equation for capacitance of the RLC branch of the resonant filter is reached:

$$C = \frac{\left(\frac{1}{Q_z} \cdot \frac{\omega_1^2}{\omega_r^2}\right)^2 + \left(1 - \frac{\omega_1^2}{\omega_r^2}\right)}{\left(1 - \frac{\omega_1^2}{\omega_r^2}\right)} \cdot C_{\text{opt}} \tag{23}$$

Also, while taking into consideration that in resonant filters $Q_z^2 \gg 1$, necessary capacitance in *RLC* branch for reactive power compensation is:

$$C \approx \left(1 - \frac{\omega_1^2}{\omega_r^2}\right) \cdot C_{\text{opt}} \tag{24}$$

If resonant frequency ω_r is adjusted according to the frequency ω_h of the harmonic which is being stifled, i.e., if discrepancy factor of the filter is $\delta = 0$, the previous equation become:

$$C \approx \left(1 - \frac{1}{h^2}\right) \cdot C_{\text{opt}} \tag{25}$$

Based on capacitance in the *RLC* filter branch and the frequency of the harmonic that needs to be stifles, using the Eq. (8) determines the inductivity in the *RLC* filter branch:

$$L = \frac{1}{\omega_r^2} \cdot C \tag{26}$$

Based on inductivity in the *RLC* filter branch and the filter quality factor, using the Eq. (9) determines the resistance in the *RLC* filter branch:

$$R = \frac{\omega_r \cdot L}{Q_z} \tag{27}$$

In the case when two higher dominant harmonics need to stifle, two parallel RLC filters with resonant frequencies ω_{r1} and ω_{r2} are necessary, and the frequencies should be equal to the frequencies of two dominant higher harmonics. Total susceptance of filter branches is:

$$B_{f1} + B_{f2} \approx \frac{\omega_1 C_1}{\left(1 - \frac{\omega_1^2}{\omega_{r1}^2}\right)} + \frac{\omega_1 C_2}{\left(1 - \frac{\omega_1^2}{\omega_{r2}^2}\right)} = \omega_1 \cdot C_{\text{opt}} \tag{28}$$

In this case, the solution for capacitance C_1 and C_2 within filter branches is not unequivocal. One of the ways to determine the filter branch parameters is for the capacitance C_{opt} to equally distribute along *RLC* branches (if frequency of the harmonics which are being stifled are close to each other, such as the fifth and seventh harmonic). Capacitance of the *RLC* branches would be:

$$C_1 \approx \left(1 - \frac{\omega_1^2}{\omega_{r1}^2}\right) \cdot \frac{C_{\text{opt}}}{2} \tag{29}$$

$$C_2 \approx \left(1 - \frac{\omega_1^2}{\omega_{r2}^2}\right) \cdot \frac{C_{\text{opt}}}{2} \tag{30}$$

The second way of determining parameters of parallel RLC filters is to assume equal active resistances in the RLC branches. In that case, along Eqs. (16), (17), (19) and (20),

additional equation which enabled determining parameters of the *RLC* branch is:

$$R_1 = R_2 \cdot \frac{\omega_{r1} \cdot L_1}{Q_z} = \frac{\omega_{r2} \cdot L_2}{Q_z} \cdot \omega_{r1} \cdot C_1 = \omega_{r2} \cdot C_2 \qquad (31)$$

Filter parameters with one resonant frequency can also be assessed based the value of reactive power which needs to be compensated optimally. In the case of monophasic consumer, capacitance in the *RLC* branch of the filter is expressed using reactive consumer power Q_{tot} which is:

$$C \approx \left(1 - \frac{\omega_1^2}{\omega_r^2}\right) \cdot \frac{Q_{\text{tot}}}{\sqrt{\sum_{k01}^{n} U_k^2} \cdot \sqrt{\sum_{k=1}^{n} \omega_k^2 U_k^2}} \qquad (32)$$

where n is the highest harmonic rank which is taken into consideration, and U_k are effective values of harmonic voltages.

The rest of the parameters of the *RLC* branches are determined using the Eqs. (17) and (18). In the case of two higher dominant harmonics which are being compensated for, reactive power is distributed along filter *RLC* branches.

In the case of three-phase system with relatively small asymmetries, equal capacitances of the filter can be assessed in phases according to basic nonactive power

Q_{tot} of the three-phase consumer:

$$C \approx \left(1 - \frac{\omega_1^2}{\omega_r^2}\right) \cdot \frac{Q_{\text{tot}}}{\sqrt{\sum_{k01}^{n} \left(U_{ak}^2 + U_{bk}^2 + U_{ck}^2\right)} \cdot \sqrt{\sum_{k=1}^{n} \omega_k^2 \left(U_{ak}^2 + U_{bk}^2 + U_{ck}^2\right)}} \qquad (33)$$

where n is the highest harmonics rank which is taken into consideration, and U_{ak}, U_{bk} and U_{ck} are effective values of the phasic harmonic voltages u_a, u_b and u_c.

Active filters are electronic converters which are programmed to conduct higher harmonics compensation. They follow injection of the no non-sinusoidal current based on which they generate current which, when superimposed with harmonic current gives a "clear" sinusoid. More complex configurations enable complete elimination of all disturbances which affect the quality of electric energy [19-24].

4 ANALYSIS OF HIGHER HARMONICS USING SIMULATION

In order to detect problems of nonlinear load, three-phase part of the electric network will be analysed where the electric arc is powered using the transformer YY junction during the welding process via six-pulse bridge unmanageable rectifier. Simulation is conducted using the MATLAB/PSB package.

Fig. 4 showcases the model of the analysed part of the three-phase electric network where it is apparent that the welding device transformer if incorporated directly into the network without higher harmonics filter.

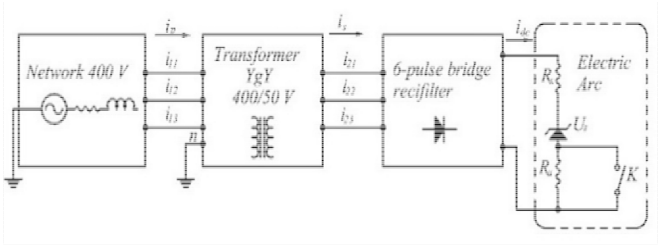

Figure 4 Analysed part of the network

Model parameters are:

Network: Voltage level: U_n = 400 V (line voltage); Phase angle of the first phase φ = 0°; Network parameters: R_s = 0,3 Ω; L_s = 0,15 mH.

Transformer (linear model): Rated power S_n = 11,5 kVA; Transfer ratio of the transformer: 400/50 V; Work resistance and reactance of the primary and secondary coil: $R_p = R_s$ = 0,003 p.u.; $X_p = X_s$ = 0,06 p.u.

Parameters of the magnetisation branch: R_m = 150 p.u.; X_m = 150 p.u.

Parameters of the electric arch model: R = 0,225 Ω.

L = 0,15 mH.

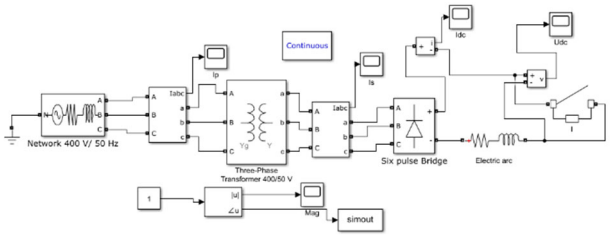

Figure 5 Simulation model of the analysed part of the network before the implementation of the network filter

Simulation model of the showcased electrical network in MATLAB is represented in Fig. 5. Simulation of the model will determine the waveform of the phase-one current at the voltage level of 400 V. After the simulation is conducted, waveform of the phase-one current at the primary side of the transformer is showcased in Fig. 3. Waveform of the *R* phase voltage and zero conductor is showcased in Fig. 5.

Fig. 6 showcases simulation model of the analysed network before higher harmonics filter implementation in MATLAB and on Figs. 9 to 12 represent the recording of transformer effect current regarding welding. Waveforms of currents and volage on the major and minor are showcased in the following pictures.

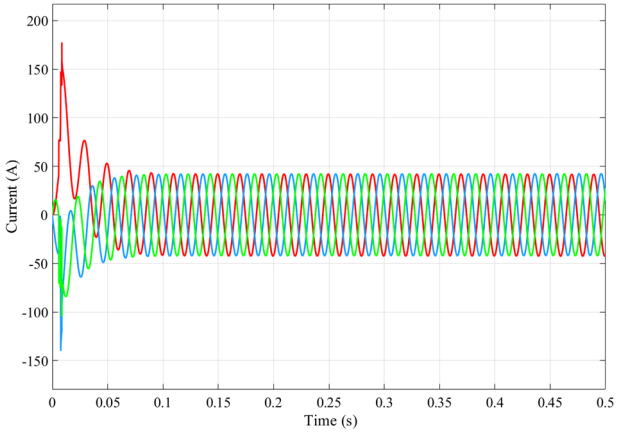

Figure 6 Waveform of primary inrush tranfformer currents after conducted by simulating transformer idling

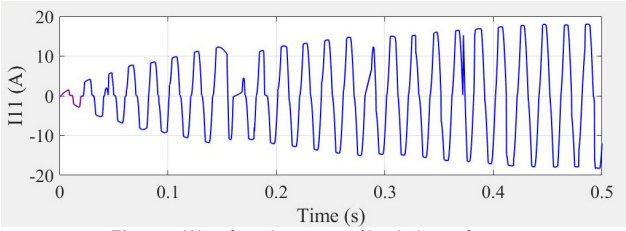

Figure 7 Waveform i_{11} current of loaded transformer

Fig. 7 represents waveform of the primary current of the loaded transformer model.

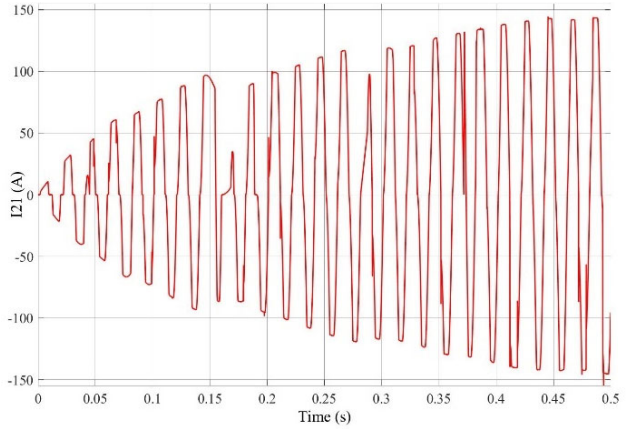

Figure 8 Waveform of the loaded transformer i_{21} secondary current

Fig. 8 show cases waveform of the secondary current model of the loaded transformer.

Harmonic contet of i_{11} current on the primary side of transformer, showcased on Fig. 9.

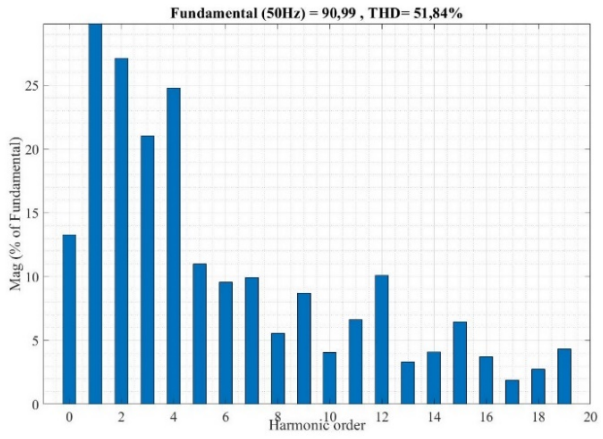

Figure 9 Harmonic content of the i_{11} current of the transformer's first phase

Based on values provided via simulation, indicator calculation of harmonic current distortion is given in the following way:

$$THDI_{11} = \frac{\sqrt{\sum_{n=2}^{\infty} I_n^2}}{I_{11}} \cdot 100\ \% = 51{,}84\ \% \tag{34}$$

4.2 Simulation Model with an Installed Filter

To showcase the effect of lessening or eliminating higher harmonics via installing a filter, on the same simulation model a three-phase filter will be dimensioned. Simulation model with one filter is shown on Fig. 10.

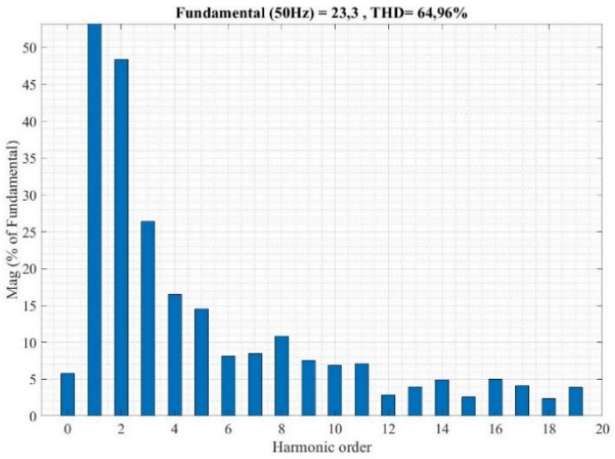

Figure 10 Harmonic content of the i_{21} transformer current

Implemented three-phase filter is dimensioned for eliminating maximal harmonic current component of phase *1* on the 400 V transformer side. Recorded waveform of the i_1 current on the primary transformer side, when one three-phase filter is implemented, is showcased on Fig. 11.

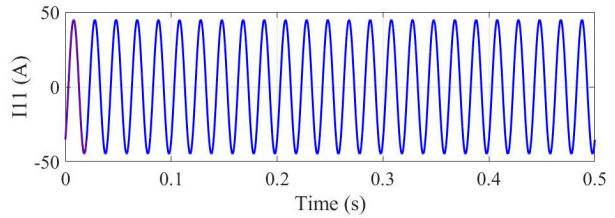

Figure 12 Waveform of the i_{11} current of the first transformer phase after implementing the filter into the simulation model

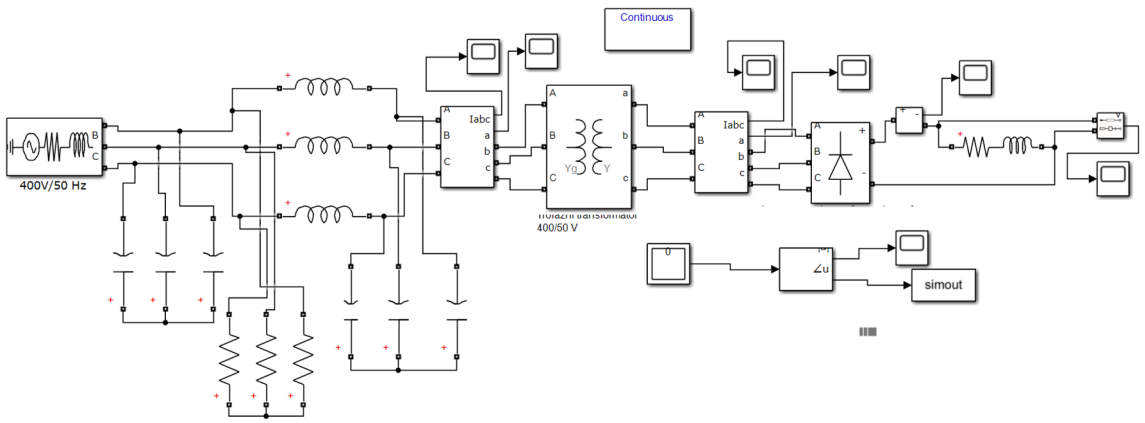

Figure 11 Simulation model of analysed part of the network after implementing the network harmonic filter

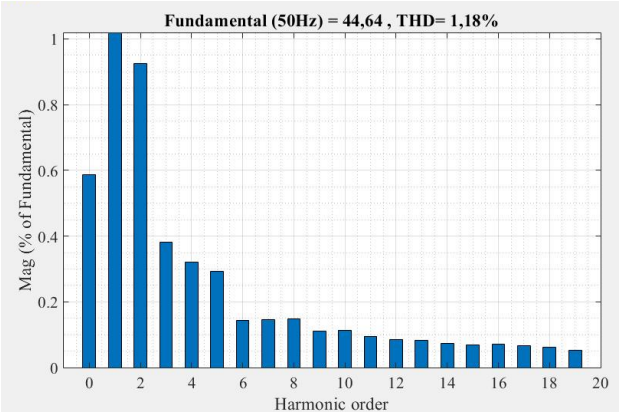

Figure 13 Harmonic content of the primary current of the transformer first phase after installing the filter the into the simulation model.

Based on the values provided by the simulation, indicator calculation of the harmonic current distortion after implementing the filter into the model is provided in the following way:

$$THDI_{11} = \frac{\sqrt{\sum_{n=2}^{\infty} I_n^2}}{I_{11}} \cdot 100\ \% = 1{,}18\ \% \qquad (35)$$

The result (35) shows that in this case the harmonic distortion is even smaller and almost eliminated.

4.3 Measured results on transformer

Fig. 14 shows waveform of measured values primary currents of three-phase transformer during loading.

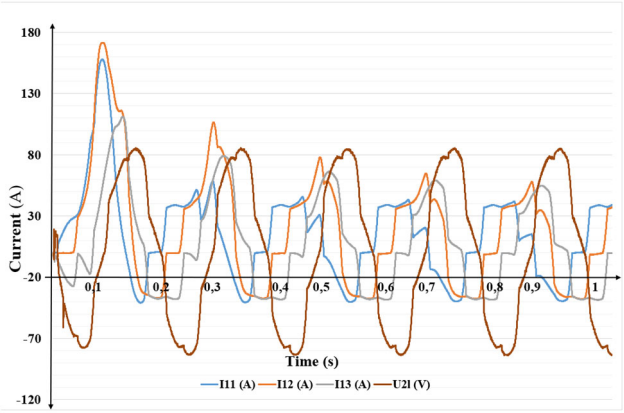

Figure 14 Waveform of the primary currents of the three-phase transformer without the filter into the measured model [21]

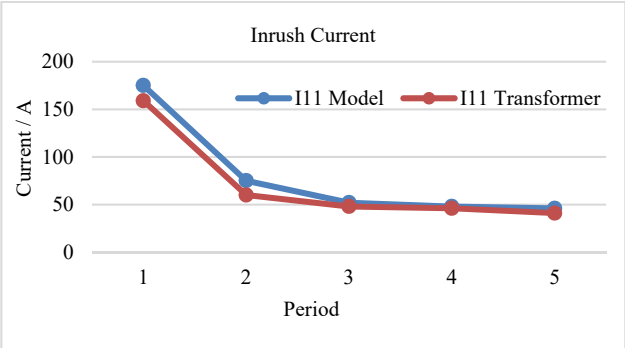

Figure 15 Maximal value of i_{11} in five periods

Fig.15 showcases maximal value of i_{11} impact currents in the first five periods of the examined model and loaded welding device transformer. The presented results that can be found on Fig. 14 deviate up to 10% in regard to the device model and measured values of transformer current.

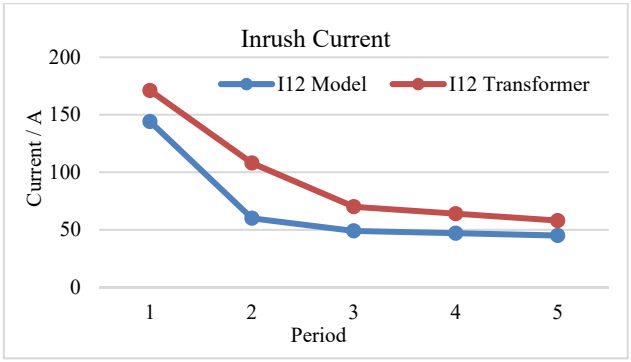

Figure 16 Maximal value of i_{12} in five periods

On Fig. 16, there are significant deviations between the device model and measured transformer values.

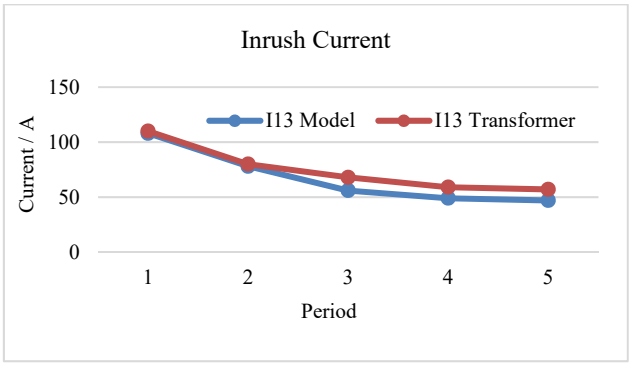

Figure 17 Maximal value of i_{13} in five periods

In Fig. 17, the presented results deviate up to 10% in regards the device model and maximal measured values on transformer currents.

5 CONCLUSION

This paper showcases simulated waveforms of three-phase transformer effect currents during incorporating the same into city network.

Simulation model in Simulink provides similar values of idling major waveforms to those under load.

Based on conducted calculations of THDI i_1 currents depending on the network topology, without filter and with two filters, comparison of harmonic distortion indicator is easily conducted:

- THDI i_1 with no filter is 51,84%
- THDI i_1 with two filters is 1,18%

It can be concluded that implementing the filter lowers the THDI, i.e., from 51,84% to 1,18% by eliminating the fifth harmonic. By implementing two filters, THDI improved even more and came to 1,18 % and it is apparent in this case that harmonic distortion is almost eliminated.

Time of 0,5 s is taken for total duration of the simulation. Harmonic current components were calculated up to the 15th harmonic and during the 25th cycle.

It can be empirically stated that higher harmonics have a negative effect on transfer power of electro-energetic lines due to increased losses in the lived. They can then cause errors in devices which are implemented to the electric current, and especially monitoring devices due to the transformer getting frequently turned on/off while welding.

Furthermore, they can cause braking of electric motors, while public lighting lamps filled with gas can have a smaller factor of usability due to higher harmonics, as well as households, which can experience flickering of Wolfram lightbulbs during the welding device utilization. In conclusion, sinusoidal waveform of voltage and current should be as clear as possible.

By comparing the model and maximal measured values of transformer currents, it can be concluded that deviations of impact current values depend on several factors, namely the nominal data of the examined transformer (working resistance of the primary and secondary coil, type of performance and core material), resistance and inductivity of the welding electrode, as well as circuit stiffness.

6 REFERENCES

[1] Katić, V. (2002). *Kvalitet električne energije- viši harmonici.* Fakultet tehničkih nauka, Edicija tehničke nauke - Monografije, Univerzitet u Novom Sadu.

[2] Ramirez, R. (1985). *The FFT - Fundamentals and Concepts*. Prentice-Hall Inc., Englewood Cliffs, New Jersey.

[3] Katić, V., Tokić, A., & Konjić, T. (2007). *Kvalitet električne energije*. Novi Sad.

[4] Lukačević, Z. (1998). *Zavarivanje*. Strojarski fakultet Slavonski Brod, Sveučilište u Osijeku, Slavonski Brod.

[5] Puklavec, A. & Domjan, S. (2002). *Pregled izvedbi izvora struje zavarivanja, Zavarivanje 45*. Društvo za tehniku zavarivanja Zagreb.

[6] Mitraković, B. (1985). *Transformatori*. Naučna knjiga Beograd, VIII izdanje.

[7] Kelemen, T., (1997). *Transformer (transformator).* Technical Encyclopedia (Tehnička enciklopedija), Zagreb, Croatia.

[8] Specht, T. R. (1951). Transformer Inrush and Rectifier Transiet Currents. *IEEE Transcantions (Power Aparatures and Systems).*

[9] Yacamni, R., Eng, C., & Abu-Nasser, A. (1986). The Calculation of Inrush Current in Three-phase transformers. *IEE Proceedings*, *133*(1).

[10] Brunke, J. H. & Frolich, K. J. (2001). Elimination of Transformer Inrush Currents by Controlled Switching, part I and II. *IEEE Transactions on Power Delivery*, *16*(2).

[11] Maljković, Z. (2011). *Transformatori*. Fakultet elektrotehnike i računarstva, Zagreb.

[12] Wokring Group 13.07, (1999). Controlled Switching of HVAC Circuit Breakers, Electra No.185.

[13] Stojkov, M. & Špoljarić, Ž. (2012). New Possibilities in Inrush Current Phenomena Analysis. *Journal of Electrical & Electronics*, *1*(3).

[14] Lin, C. E., Cheng, C. L., & Huang, C. L. (1993). Investigation of Magnetizing Inrush Current in Transformers. *IEEE Transactions on Power Delivery*, *8*(1).

[15] Špoljarić, Ž. (2016) *Simulacijski model energetskih transformatora za analizu struje uklopa*. Doktorska disertacija, Sveučilište J. J. Strossmayera u Osijeku, FERIT.

[16] Katić, V. (2002). *Kvalitet električne energije - viši harmonici*. Sveučilište u Novom Sadu, Fakultet tehničkih nauka.

[17] Arrillaga, J., Bradley, D., & Podger, P. (1985). *Power System Harmonics*. John Wiley & Sons, Chichester.

[18] Graovac, D., Katić, V., & Rufer, A. (2000). Power Quality Compensation Using Universal Power Quality Conditioning System. *IEEE Power Engineering Review*.

[19] http://ees.etf.bg.ac.rs/predmeti/27/KEE10_Prigusenje%20visih%20harmonika.pdf

[20] Špoljarić, Ž., Jerković, V., & Stojkov, M. (2012). Measurement System for Transformer Inrush Current Higher Harmonics Determination. *The 23rd DAAAM International Symposium Intelligent Manufacturing and Automation*.

[21] Petrović, I., Stojkov, M., Samardžić, I., & Marić, P. (2017). Inrush current of welding machine. *9. International Scientific professional conference; Engineering technologies in manufacturing of welded contractions and products.*

[22] Stojkov, M. & Špoljarić, Ž. (2012). New Possibilities in Inrush Current Phenomena Analysis. *Journale of Electrical & Electronics*, *1*(3).

[23] Crnković, D., Vrandečić, N., & Stojkov, M. (2010). Transiets No-Load Condition of Power Transformer 20/0,4 kV. *Technical Gazzete*, *17*(2), 179-183.

[24] Vukobratović, M., Marić, P., Nikolovski, S., & Glavaš, H. (2017). Distributed Generation Harmonic Interaction in the Active Distribution Network. *Technical Gazette*, *25*(6), 1720-1730. https://doi.org/10.17559/TV-20171025123650

[25] Bulatović, S., Aleksić, V, Milović, Lj., & Zečević, B. (2022). Experimental Determination of the Critical Value of the J-Integral that Refers to the HSLA Steel Welded Joint. *Technical Gazzete*, *30*(1), 148-147. https://doi.org/10.17559/TV-20220419093052

[26] Sehrili, E. & Cetinceviz, Y. (2022). Comparasion of Average Curent Controlled PFC SEPIC and CUK Cinverter Feeding Current Controlled SRM. *Technical Gazette*, *29*(6), 1789-1795. https://doi.org/10.17559/TV20181108110207

[27] Marappan, S., Kasirajan, L., & Shanmugam, V. (2022). Friction Stir Welding Experiments on A31B Alloy to Analise Mechanical Propertis and Optimize Process Variables by TOPSIS Method. *Tehnical Gazette*, *29*(6), 1923-1930. https://doi.org/10.17559/TV-20220309035350

Contact information:

Ivan PETROVIĆ, mag. ing. el.
(Corresponding author)
Saint Jean Industries d.o.o.,
35000 Slavonski Brod, Croatia
E-mail: ipetrovic81@gmail.com

Marinko STOJKOV, PhD
University of Slavonski Brod,
Mechanical Engineering Faculty,
Trg Ivane Brlić Mažuranić, 35000 Slavonski Brod
E-mail: mstojkov@unisb.hr

Damir ŠLJIVAC, PhD
J. J. Strossmayer University of Osijek,
Faculty of Electrical Engineering,
Computer Science and Information Technology Osijek,
Kneza Trpmira 2B, 31000 Osijek, Croatia
E.mail: damir.sljivac@ferit.hr

Mijat SAMARDŽIĆ, mag. ing. mech.
University of Slavonski Brod,
Mechanical Engineering Faculty,
Trg Ivane Brlić Mažuranić, 35000 Slavonski Brod
E-mail: msamardzic@gmail.com